



Contents lists available at <http://www.jmsse.org/> & <http://www.jmsse.in/>

Journal of Materials Science and Surface Engineering



Surface Composites Defects of Al/Al₂O₃ Metal Matrix Fabricated by Friction Stir Processing

Essam B. Moustafa¹, Samah Mohammed², Sayed Abdel-Wanis², Tamer Mahmoud², El-Sayed El-Kady²

¹Mechanical Engineering Department, Faculty of Engineering, King Abdul-Aziz University, K.S.A.

²Mechanical Engineering Department, Shoubra Faculty of Engineering, Benha University, Egypt.

Article history

Received: 07-Jan-2017

Revised: 31-Jan-2017

Available online: 20-Mar-2017

Keywords:

FSP,
Defects,
Surface,
Composite

Abstract

In the current work AA2024 alloy has been reinforced with alumina nano particles using friction stir processing with three multiple passes. The heat generated during FSP is varied depend on the processing parameters speeds, a furthermore number of passes. Defects arise through all fabrication process have been detected by macroscopic examination. The result revealed that multi-pass FSP improves the surface composite homogeneity though dispersion of Al₂O₃ nano particles in the metal matrix composite.

© 2017 Science IN. All rights reserved

Introduction

Friction stir processing is considered the most advanced technique used to develop modified surfaces. The process controlled by processing parameters such as tool rotation speed, travel speed, tool shaped design, tool tilt angle and numbers of passes are performed [1-3]. Processing parameters control the amount of heat generated in the specimen, the interaction between the rotating tool and specimen generates heat due to friction action and plastic deformation. Insufficient heat input or inadequate/improper plastic flow causes many Defects such as the tunnel, cavities and pinholes could form during friction stir processing [4]. Many researchers have discussed the relation between the process parameters and the quality of processed metals according to [5-9]. The heat generated in Stirring Zone effect on material flow and consequently, affects the mechanical and tribological properties [10]. The heat-generated process is one of the most important aspects of the FSP investigation. The study and understanding of the heat transfer process can be useful in evaluating and predict the thermal cycles of the processed surfaces [11]. There are a few published mathematical and analytical models with the different approach are calculating and evaluating the amount of heat generated during FSW and FSP [12-15].

The main aims of the current work is to investigate the Effect of processing parameters on the defects formed during friction stir processing AA2024-Al₂O₃ metal matrix Nano composite surface, Moreover the study the effect of processing parameters on the heat generation that influence on the quality of the fabricated surface composite metal.

Experimental

In the current study, the base material has been used is AA 2024-O sheets with 4 mm thickness are fabricated with Al₂O₃ nanoparticles using friction stir processing in order to

develop a surface composite layer. The chemical composition of the as-received material is given in Table 1.

Table 1: Chemical composition of the as received AA2024 alloy (weight %)

Element	Cu	Mg	Mn	Zn	Fe	Si	Pb	Sn	Al
%	4.89	1.45	0.62	0.16	0.12	0.11	0.02	0.01	remain

Material preparation

The base metal sheets are prepared into square plates (150mm*150 mm) then, three Straight grooves with 5mm width and 2mm thickness, have been machined in each plate using milling machine (*Bridgeport* Vertical Milling Machine). Nano particles Al₂O₃ with 30 nanometer average diameter been filled in the base metal grooves. The milling machine is adapted for the FSP experiments. The fabrication process on the surface is shown in Fig. 1.

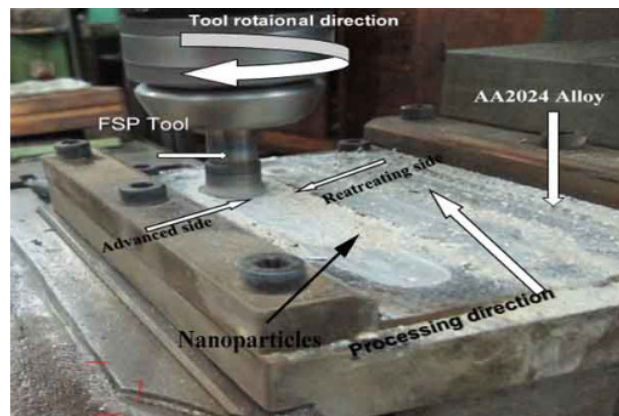


Figure1: Surface composite fabrication process using FSP technique

Temperature measurement

The temperature during friction stir processing was measured using a thermal camera (FlukeTIS10) in order to record the maximum temperature in different processing conditions as shown in Fig. 2.

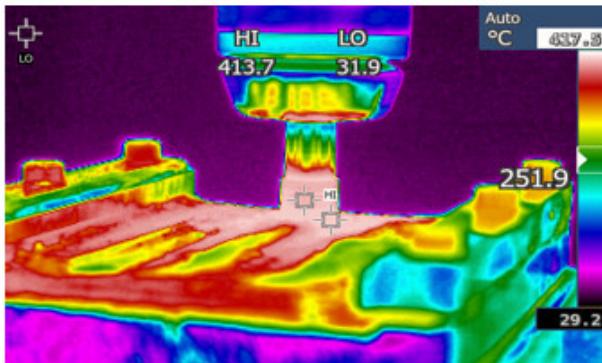


Figure 2: Temperature measurement during FSP using thermal camera

Macro structure preparation and examination

The samples are prepared to macrostructure examination which, grinding using (Metasery Grinder 2000) machine then etched with classical Keller's reagent (2 ml HF(48%) + 6 ml HNO₃+ 91 ml distilled water) at room temperature until desired contrast is obtained. Macrostructure analysis is performed to understand the influences caused by the process parameters. The surfaces of specimens are scanned using high-resolution scanning 2400 dpi (hp scan jet 300) in order to examine the shape of processed zone during FSP.

Results and Discussion

During FSP, the heat generated by the friction and stirring action causes the materials flow around the tool pin, and therefore it considered the main factor that affects the formation of defects. Regarding the pervious investigators, [16-17]. The three defects are formed during FSP. First, tunnels or groove that produced due to insufficient heat input. Second, a large mass of flash to be ejected outside the stirring zone. Third, pin hole and cavities formed due to a non-uniform temperature distribution and discontinuous material flow, so that the processing parameters are responsible for identifying the processing conditions with defect free.

Effect of processing parameters

Increasing the rotational speed leads to an excessive heat input inside the nugget zone, so that it has become wider and flatter. A large amount of frictional and plastic-work heat is produced and because of easy material flow, a bigger nugget is formed. The first pass in all processing conditions has cavities, tunnels and grooves along the processing path, as shown in the Fig. 3.

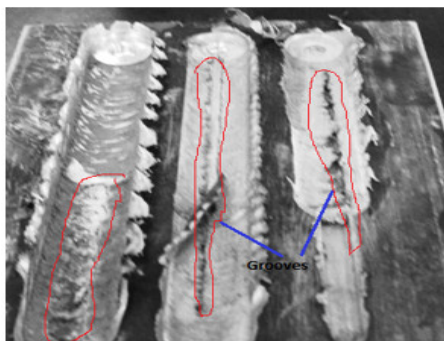


Figure 3: Longitudinal grooves and cavities formed in the FSP first pass

Thus can be attributed to the alumina Nano particles in the first pass cannot be dispersed homogenously in the first pass. It is observed that in the first pass formation of flashes that ejected outside the stirring zone, this is attributed to low heat input and low frictional heat and plasticized metal produced during the process as shown in Fig. 4.

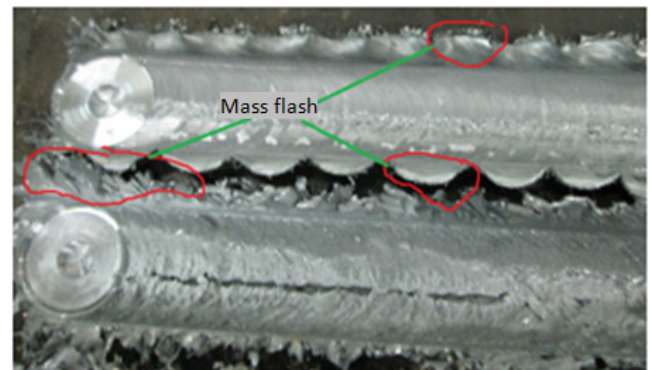


Figure 4: Mass flash formation during FSP first pass

Increasing traverse speed leads to a decrease in the size of the nugget zone and increase the roughness of the surface and the amount of the material removed increase (flashes). Figure 5 shows the relation between travel speed and heat generated during FSP through different four-tool rotation speed. Higher rotation speed with higher travel speed produced unsuccessfully surfaces composite as shown in Fig. 6, despite performed multi-pass processing surface. Figure 7 shows the macrographs section in the stirred zone, among the four-tool rotation speeds used to fabricate the surface composite. The rotation speeds of 900 rpm and 1120 rpm are produced defect-free surface in the second and third pass. At higher speed such as 1400 rpm and 1800 rpm, the defects appear lower volume with increasing number of passes, but still having defects in most processed passes that marked in red circular.

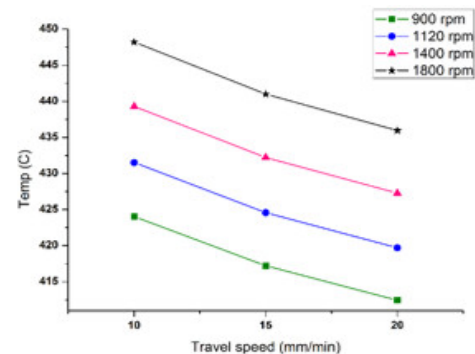


Figure 5: Effect of processing parameter (rotation and travel) speeds on the heat generation during FSP

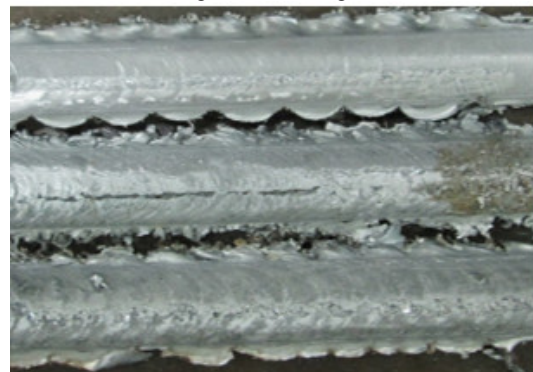


Figure 6: Unsuccessfully FSPed samples at higher speed with multiple passes 1800 rpm rotation speed at 10 mm/min travel speed

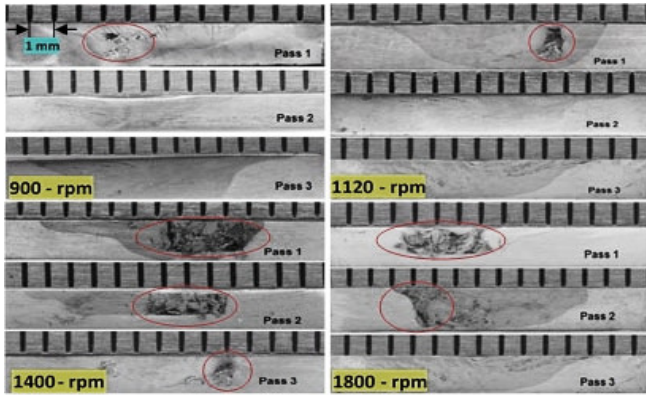


Figure 7: The macrographs section in the stirred zone at 10 mm/min travel speed and different four rotation speeds three passes number during

Increasing travel-processing speed causes a gradually improving in the grain size refinement at the surface composite, due to increasing the ratio (r) of travel speed to rotational speed. Appearance of imperfections and defects were reduced at higher rotation speed in case of 1400 rpm and 1800 rpm with 20 mm/min travel speed as shown in Fig. 8. The heat generation increasing exponentially with respect to the ratio (r) according to the empirical equation (1), driven from the measured data as shown in Fig. 9. While decreasing the speeds ratio it causes an irregular stirring action in the material flow, the results are consistent with [18].

$$T_{max} = \frac{T_{melt}}{2} \times r^{-b} \quad (1)$$

Where,

$[T_{melt}]$ is the melting point of base metal;

$[r]$ Travel speed to rotation speed ratio ($\frac{v}{\omega}$).

$[b]$ Constant factor [0.05-0.06]

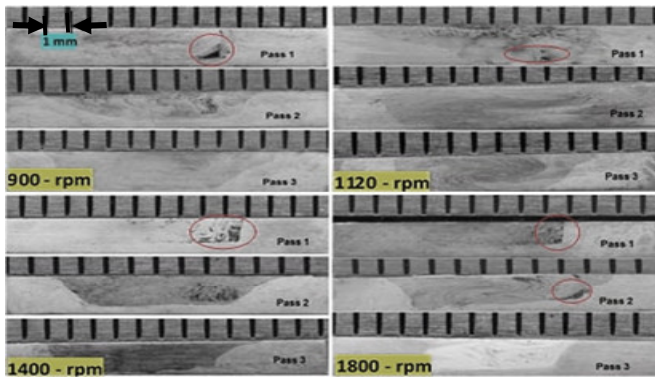


Figure 8: Defect free in the processed surface due to increasing the travel speed for 20 mm/min and number of FSP passes

It is noted that through experiments, Al₂O₃ nanoparticles cannot dispersed well in the first processing pass, although the very thick surface appear homogenous, but small cavities found in lower layer surface of matrix. Another observation, the reinforcement particles can disperse well as the rotation speed not exceeds 1200 rpm. The heat generation (r) depends on the ratio between rotation speed and linear processing speed; consequently, the defects arise from insufficient heat generation required for homogenization the nanoparticles with the base metal alloy during FSP.

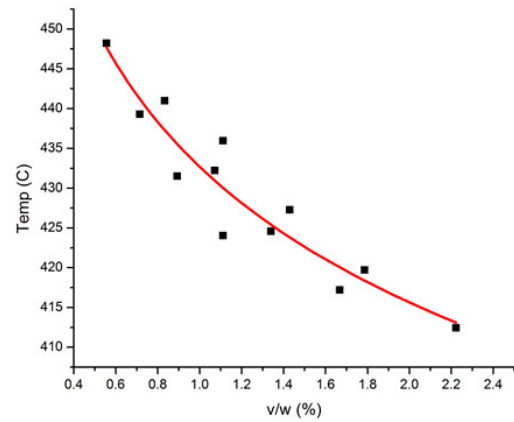


Figure 9: Maximum temperature with respect to speed ratio (v/ω)

Conclusions

In this paper the stirring zone shape determine the historical friction stir processing parameters.

- Heat generation during FSP has a maximum at lower traverse speed with higher rotation speed.
- The number of pass play an important role in the dispersion of alumina particles in the metal matrix during FSP furthermore it cause a homogeneous surface composite.
- Increasing number of passes reduces the defects formed in the first pass. The optimum conditions to enable the Al₂O₃ nano particles to be dispersed well in the metal matrix surface were observed at 900 rpm and 1120 rpm with 20 mm/min travel speed.

References

1. Emad Salari, Mohammad Jahazi, A. K. ., H. G.-N., "Influence of tool geometry and rotational speed on mechanical properties and defect formation in friction stir lap welded 5456 aluminum alloy sheets," *Materials and Design*, vol. 58, p. 381–389, 2014.
2. D. Trimble, G. O'Donnell and J. Monaghan, "Characterisation of tool shape and rotational speed for increased speed during friction stir welding of AA2024-T3," *Journal of Manufacturing Processes*, vol. 17, p. 141–150, 2015.
3. Rui Yang, Zhenya Zhang, et al., "Effect of multi-pass friction stir processing on microstructure and mechanical properties of Al3Ti/A356 composites," *Materials Characterization*, vol. 106, p. 62–69, 2015.
4. K. Elangovan and V. Balasubramanian, "Influences of pin profile and rotational speed of the tool on the formation of friction stir processing zone in AA2219 aluminium alloy," *Materials Science and Engineering A*, vol. 459, p. 7–18, 2007.
5. S. Rajakumar and V. Balasubramanian, "Establishing relationships between mechanical properties of aluminium alloys," *Materials and Design*, vol. 40, p. 17–35, 2012.
6. Devaraju, A. Kumar and A. Kumaraswamy, "Influence of reinforcements (SiC and Al₂O₃) and rotational speed on wear and mechanical properties of aluminum alloy 6061-T6 based surface hybrid composites produced via friction stir processing," *Materials and Design*, vol. 51, p. 331–341, 2013.
7. K. Hussain and S. A. P. Quadri, "Evaluation of parameters of friction stir welding for aluminum AA6351 alloy," *International Journal of Engineering Science and Technology*, vol. 2(10), pp. 5977–5984, 2010.
8. P. D. Edward and M. Ramulub, "Material flow during friction stir welding of Ti-6Al-4V," *Journal of Materials Processing Technology*, vol. 218, p. 107–115, 2015.
9. T. Dickerson, J. H. Hattel and H. N. Schmidt, "Material flow in butt friction stir welds in AA2024-T3.," *Acta Materialia*, vol. 54, p. 1199–1209, 2006.
10. S. N. S. Y.J. Kwon, "Mechanical properties of fine-grained aluminum alloy produced by friction stir process," *Scripta Materialia*, vol. 49, p. 785–789, 2003.

11. M. Song and R. Kovacevic, "Thermal modeling of friction stir welding in a moving coordinate system and its validation," *International Journal of Machine Tools & Manufacture*, vol. 43, p. 605–615, 2003.
12. R. Mishra and . Z. Ma, "Friction stir welding and processing," *Materials Science and Engineering*, vol. 50, p. 1–78, 2005.
13. H. Schmidt, J. Hattelx and J. Wert, "An analytical model for the heat generation in Friction Stir Welding," *Modeling Simul. Mater. Sci. Eng.*, vol. 12, no. 1, pp. 143-157, 2004.
14. R. Nandan, "Three-dimensional heat and material flow during friction stir welding of mild steel," *Acta Materialia*, vol. 55, pp. 883-895, 2007.
15. H. Bisadi, A. Tavakoli, M. T. Sangsaraki and K. T. Sa, "An analytical model for the heat generation in friction stir welding," *Materials and Design*, pp. 80-88, 2013.
16. C.-y. Yang, "Inverse determination of heat input during the friction stir welding process," *International Journal of Heat and Mass Transfer*, vol. 76, p. 411–418, 2014.
17. Askari, A., Silling, S and London, B, "Modeling and analysis of friction stir welding processes," in *Proceedings of Symposium on Friction Stir Welding and Processing*, 2001.
18. M. Narimani, B. Lotfi and Z. Sadeghian, "Investigating the Effect of Tool Dimension and Rotational Speed on Microstructure of Al-B4C Surface Composite Layer Produced by Friction Stir Processing (FSP)," *Journal of Advanced Materials and Processing*, vol. 3, pp. 61-70, 2015.

